J. Plasma Physics (2013), vol. 79, part 6, pp. 1125–1128. © Cambridge University Press 2013
doi:10.1017/S0022377813001098

How to quantify solid–liquid phase transition: Lennard–Jones system case study

BORIS A. KLUMOV

High Temperature Institute, Moscow 123060, Russia
(klumov@ihed.ras.ru)

(Received 3 September 2013; revised 3 September 2013; accepted 6 September 2013; first published online 18 October 2013)

Abstract. In this paper we analyzed different measures, characterizing the melting of Lennard–Jones solid, and associated with the properties of both the translational and the orientational local order. It has been shown that the most sensitive indicator of melting is the cumulant of the probability distribution function over w_6 bond-order parameter. The criterion of melting based on the indicator is proposed; the criterion can be used for any solids, having fcc/hcp types of symmetry.

1. Introduction

Melting and crystallization of matter are of fundamental interest in condensed matter physics. Microscopic nature of melting is not fully understood yet even for simple systems, like Lennard—Jones (LJ) one, although it is well understood in numerous experimental and theoretical investigations that the physical and mechanical properties of condensed matter are determined primarily by the short-range order of atoms. The main goal of this paper is to find melting indicators that are very sensitive to phase transition. The short-range order is usually studied by analyzing the radial behavior of the pair correlation function averaged over the angular distribution of particles (radial distribution function (RDF)). Here, we also consider the properties of orientational order of LJ particles near the melting transition (Steinhardt et al. 1983; Nose and Yonezawa 1986; Mitic et al. 2008; Klumov 2010, 2013; Klumov et al. 2011) to quantify the solid–liquid transition (e.g. Avinash and Shukla 2011). One notes that melting indicators help in predicting melting, but give no explanation why the crystal melts at corresponding value of the indicator. Explanations can be found in microscopic details of particles correlations not included in the RDF, in particular multi-particles correlations. These details are very challenging for real experiments, but can be obtained at the moment by using computer simulations only. Below we consider in detail how the translational and orientational local orders vary in the vicinity of the melting transition of a LJ system to construct the most efficient indictors of the melting.

2. Numerical procedure

We use the common expression for the LJ potential in dimensionless form: $U_{\mathrm{LJ}}(r) = 4(r^{-12} - r^{-6})$ and NVT (constant particle number N, volume V, and temperature T) ensemble of particles (with $N = 4\times10^3$) arranged in a cubic box of size L with the periodic boundary conditions. Initially (at low reduced temperatures $T^* \sim 0.5$ and $\rho \simeq 1$) particles form the face centered cubic (fcc) crystal; then the system is heated by step-wise way by a small value $\delta T^* \simeq 10^{-2}$ and equilibrated configurations are used to define the structural properties. Here, the standard molecular dynamics method with the Verlet algorithm and Langevin thermostat (e.g. Klumov 2013) is used to calculate the particle configurations.

2.1. RDF-associated melting indicators

Let us start to consider the structural properties of LJ system in the vicinity of melting transition by analyzing the radial distribution function $g(r)$ (RDF). Figure 1 shows the typical behavior of $g(r)$ versus temperature T^* and distance r. The change in the RDF at melting is rather sharp, with only a narrow temperature range where there is a crossover between crystal and liquid. One can see that between $T^* \simeq 1$ and the melting temperature $T_m^* \simeq 1.65$ there are remarkable changes in the RDF of the crystal: the additional maxima between the main maxima in the RDF become undetectable. These additional maxima describe fine details of the fcc lattice. The disappearance of the additional maximum between the first and the second main maximum is illustrated by inset in Fig. 1. We note that the sharp breaking of $g(r)$ (at $T^* \simeq 1.6$) is clearly seen *at all spatial scales*. It means, in part, that the melting transition can be considered at the *local order level*. Several approximate approaches have been proposed to locate the melting point of different substances. This includes phenomenological criteria for freezing and melting, like e.g. Raveché-Mountain-Streett criterion (Raveché et al. 1974) and others, including dynamical criterions as well. Figure 2 shows temperature dependencies of some melting indicators of a LJ system; $g(r)$ variations in the considered temperature range are shown in the inset. The plotted are the inverted Raveché parameter $R^{-1} = g_{\max}/g_{\min}$, which is the first maximum of $g(r)$ to the first non-zero $g(r)$ minimum ratio, parameter $g_{\min}$,

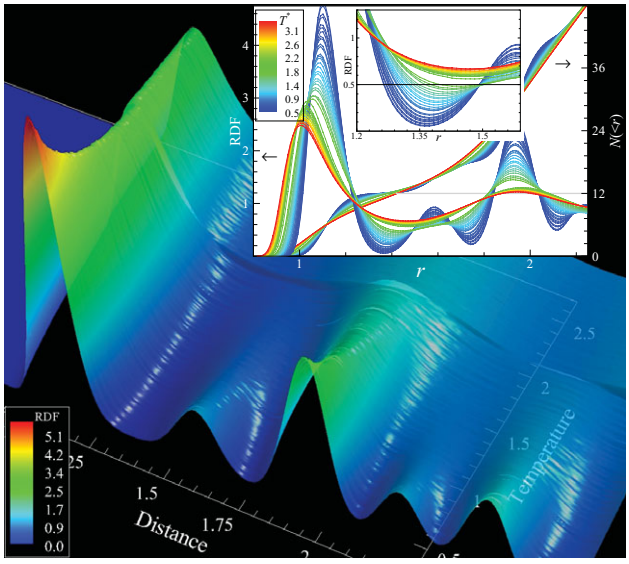

Figure 1. (Color online). Melting of Lennard–Jones system. The radial distribution function $g(r)$ is plotted versus distance r and reduced temperature T^*. The dependence is color-coded by the value of $g(r)$. Sharp change of $g(r)$ at $T^* \simeq 1.6$ occurring at all spatial scales corresponds to the melting of the system. Insets show in fine detail the behavior of $g(r)$ in the vicinity of the melting transition. The curves are color-coded by T^* value. Cumulative measure $N(<r) \equiv \int_0^r 4\pi r^2 g(r) dr$ (mean number of particles in a sphere of radius r) is also plotted at the same temperatures as $g(r)$. Additionally, modification of the first non-zero minimum of $g(r)$ is shown in detail. Reduced density of LJ system is $\rho^* = 1$.

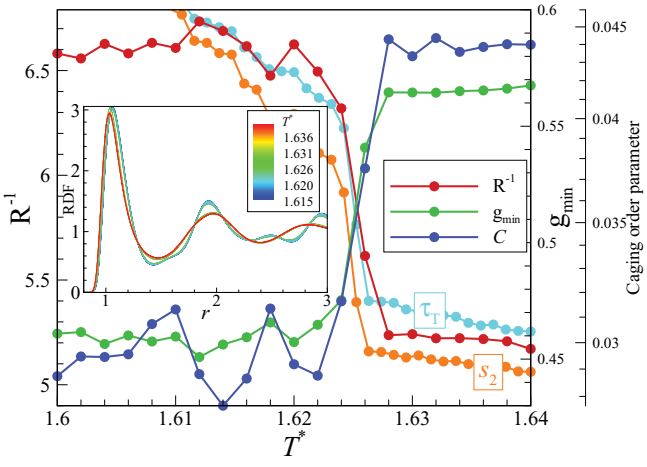

Figure 2. (Color online). Melting indicators of Lennard–Jones system versus reduced temperature. Plotted are parameters $R^{-1} = g_{\max}/g_{\min}$ (red line), $g_{\min}$ (green line), bond-breakage parameter $\mathscr{C}$, translational order parameter τ_T, and excess of pair entropy s_2. Inset shows variations of $g(r)$ in the range of considered values of temperature T^*. Reduced density is $\rho^* = 1$.

and translational order parameter τ_T defined from the expression $\tau_T \propto \int_0^{r_c} |(g(r)-1)| dr$, where r_c is distance of the order of a few interparticle distances (Truskett et al. 2000; Errington et al. 2003) and excess of pair entropy s_2 defined from $s_2 \propto \int (g(r) ln(g(r)) - g(r) + 1) d\mathbf{r}$ (e.g. Errington et al. 2003). Additionally, the bond-breakage parameter $\mathscr{C}(T^*)$, defined as an averaged loss rate of neighboring particles, is plotted in Fig. 2. All plotted measures reveal nearly the same relative variations in the range of the melting transition; that makes these parameters to be good candidates for quantification of the order/disorder in LJ system.

2.2. *Orientational local order at melting*

To define the local orientational order of LJ system we use the bond-order parameter method (Steinhardt et al. 1983), which has been widely used in the context of condensed matter physics, hard sphere systems, complex plasmas, colloidal suspensions, etc. (e.g, Gasser et al. 2001; Klumov 2010, 2013; Khrapak et al. 2012; Klumov et al. 2011). Within the method we calculate the bond-order parameters q_{lm} for each ith particle by $q_{lm}(i) = N_{\rm nn}^{-1} \sum_{j=1}^{N_{\rm nn}} Y_{lm}(\theta_j, \phi_j)$, where $Y_{lm}(\theta, \phi)$ are the spherical harmonics, and θ, ϕ are the polar and the azimuthal angles of jth neighboring particle, respectively. By using values of q_{lm}, it is easy to calculate the rotational invariants of the second q_l and third w_l orders. Calculated rotational invariants q_i, w_i are then compared with those for ideal lattices. Here, we are specifically interested in identifying face-centered cubic (fcc), hexagonal close-packed (hcp), and icosahedral (ico) lattice types, therefore use the invariants q_l, w_l calculated using the fixed number of nearest neighbors: $N_{\rm nn} = 12$ (e.g. Klumov 2010). A particle whose coordinates in the four-dimensional space (q_4, q_6, w_4, w_6) are sufficiently close to those of the ideal fcc (hcp, ico) lattice is counted as fcc-like (hcp-like, ico-like) particle. The values of q_l and w_l for the considered lattices are shown in Table 1. Note that values of q_l for odd l are non-zero for the hcp crystal only (e.g. $q_l^{\rm hcp} \approx 0.08, 0.25, 0.31, 0.13, 0.12$ for $l = 3, 5, 7, 9, 11$, respectively).

By calculating the bond-order parameters, it is easy to identify disordered (liquid-like) phase too (for instance, such particles have mean bond-order parameter $q_6^{\rm liq} \simeq N_{\rm nn}^{-1/2} \simeq 0.29 \ll q_6^{\rm fcc/hcp/ico}$, where $N_{\rm nn} = 12$). By varying the number of nearest neighbors $N_{\rm nn}$ and rank l of bond-order parameter, it is possible to identify any lattice type (including quasicrystalline particles and distorted hcp/fcc/ico modifications) existing in the system (e.g. by using $N_{\rm nn} = 8$ and 14, it is easy to identify the first and the second shells of the body centered cubic (bcc) lattices with using just q_4 and q_6 order parameters, etc.). Figure 3 shows typical temporal variations of parameters q_4, q_6, and w_6 for solid-like and liquid-like LJ systems in the vicinity of the melting transition; strong fluctuations of the parameters make it clear to use the probability distribution functions (PDF) taken over q_l and w_l values $-P(q_l)$ and $P(w_l)$ to characterize the solid–liquid transition of different close-packed solids (Klumov 2010, 2013; Klumov et al. 2011; Mitic et al. 2013). The cumulative PDFs C_q^l and C_w^l associated with the $P(q_l)$ and $P(w_l)$ (e.g. $C_q^l(x) \equiv \int_{-\infty}^{x} P(q_l) dq_l$) are used to construct the melting indicators; for instance, it can be the value $q_6^{\rm hh}$ defined from the expression $C_{q_6}^l(q_6^{\rm hh}) = 1/2$.

https://doi.org/10.1017/S0022377813001098 Published online by Cambridge University Press

Table 1. Values of q_l and w_l in the perfect crystals.

System	NN	q_4	q_6	q_8	q_{10}	q_{12}	w_4	w_6	w_8	w_{10}	w_{12}
fcc	12	0.19	0.58	0.4	0.4	0.6	−0.16	−0.013	0.06	−0.09	0.09
hcp	12	0.1	0.49	0.32	0.32	0.56	0.13	−0.012	0.05	−0.08	0.1
ico	12	0	0.66	0	0.36	0.59	−0.16	−0.17	0.06	−0.094	0.1
bcc	8	0.5	0.63	0.2	0.65	0.41	−0.16	0.013	0.06	−0.09	0.029
bcc	14	0.036	0.51	0.43	0.2	0.4	0.13	3.2×10^{-3}	0	0.018	0

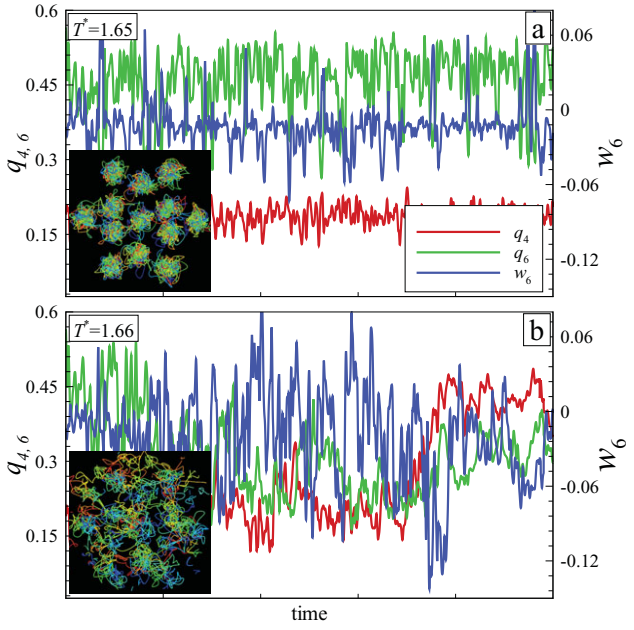

Figure 3. (Color online). Temporal variations of bond-order parameters q_4 (red line), q_6 (green line), and w_6 (blue line) for solid-like (a) and liquid-like (b) Lennard–Jones system in the vicinity of melting transition. Insets show trajectories of neighboring particles. Reduced density is $\rho^* = 1$.

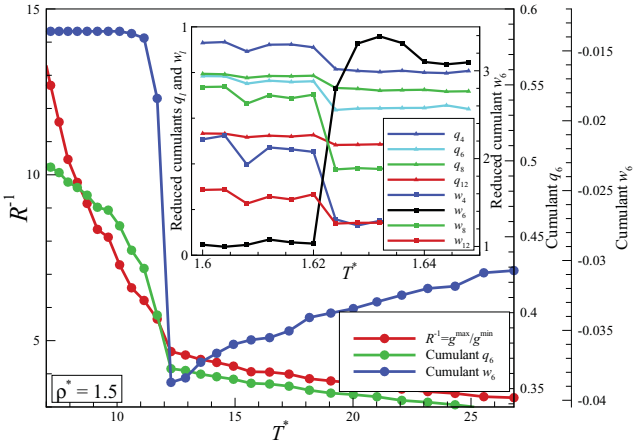

Figure 4. (Color online). Melting indicators of Lennard–Jones system against reduced temperature T^* (at $\rho^* = 1.5$). Plotted are the parameter $R^{-1} = g_{max}/g_{min}$ (red line), the cumulants of PDF over q_6 (green line) and w_6 (blue line) bond-order parameters. Inset shows the temperature dependencies of different reduced cumulants q_l and w_l (normalized to those of fcc lattice) in the vicinity of the melting transition (taken at $\rho^* = 1$). It is clearly seen that the w_6-associated cumulant is the most sensitive indicator of melting.

Other cumulants q_l^{hh} and w_l^{hh} are calculated by the same way. Figure 4 shows different indicators of melting as a function of reduced temperature T^*. It is clearly seen that the measure w_6^{hh} is the most sensitive indicator of melting; the measure changes explosively in the vicinity of the transition.

To conclude, we considered different indicators of melting of LJ system associated with both translational and orientational local order properties. It has been shown that the measure w_6^{hh} is very sensitive to the melting-induced breakage of the local orientational order; it makes the measure to be a nice melting indicator, which can be used to quantify the order/disorder transition for any close-packed solids.

Acknowledgements

The paper is devoted to the memory of Professor Padma Kant Shukla. I thank Anna and Igor Fateev for their hospitality during my stay in Odessa. This study was also partly supported by the Presidium and Division of Physical Sciences of the Russian Academy of Sciences; the Ministry of Education and Science of the Russian Federation; and the Russian Foundation for Basic Research, Projects No. 13-02-00913 and 13-02-01099.

References

Avinash, K. and Shukla, P. K. 2011 Phase coexistence and a critical point in ultracold neutral plasmas. *Phys. Rev. Lett.* **107**, 135002.

Errington, J. R., Debenedetti, P. G. and Torquato, S. 2003 Quantification of order in the Lennard–Jones system. *J. Chem. Phys.* **118**, 2256–2263.

Gasser, U., Weeks, E. R., Schofield, A., Pusey, P. N. and Weitz, D. A. 2001 Real-space imaging of nucleation and growth in colloidal crystallization. *Science* **292**, 5515.

Khrapak, S. A., Klumov, B. A., Huber, P., Molotkov, V. I., Lipaev, A. M., Naumkin, V. N., Ivlev, A. V., Thomas, H. M., Schwabe, M., Morfill, G. E., Petrov, O. F., Fortov, V. E., Malenchenko, Y. and Volkov, S. 2012 Fluid-solid phase transitions in three-dimensional complex plasmas under microgravity conditions. *Phys. Rev.* E **85**, 066407.

Klumov, B. A. 2010 On melting criteria for complex plasma. *Phys.-Usp.* **53**, 1053.

Klumov, B. A. 2013 Structural features of a Lennard–Jones system at melting and crystallization. *JETP Lett.* **97**, 327–332.

Klumov, B. A., Khrapak, S. A. and Morfill, G. E. 2011 Structural properties of dense hard sphere packings. *Phys. Rev.* B **83**, 184105.

https://doi.org/10.1017/S0022377813001098 Published online by Cambridge University Press

Mitic, S., Klumov, B. A., Konopka, U., Thoma, M. H. and Morfill, G. E. 2008 Structural properties of complex plasmas in a homogeneous dc discharge. *Phys. Rev. Lett.* **101**, 125002.

Mitic, S., Klumov B. A., Khrapak, S. A. and Morfill, G. E. 2013 Three dimensional complex plasma structures in a combined radio frequency and direct current discharge. *Phys. Plasmas* **20**, 043701.

Nose, S. and Yonezawa, F. 1986 Isothermal-isobaric computer simulations of melting and crystallization of a Lennard—Jones system. *J. Chem. Phys.* **84**, 1803.

Raveché, H. J., Mountain, R. D. and Streett, W. B. 1974 Freezing and melting properties of the Lennard—Jones system. *J. Chem. Phys.* **61**(1), 1970–1984.

Steinhardt, P. J., Nelson, D. R. and Ronchetti, M. 1983 Bond-orientational order in liquids and glasses. *Phys. Rev.* B **28**, 784.

Truskett, T. M., Torquato, S. and Debenedetti, P. G. 2000 Towards a quantification of disorder in materials: Distinguishing equilibrium and glassy sphere packings. *Phys. Rev. E.* **62**, 993–1001.

https://doi.org/10.1017/S0022377813001098 Published online by Cambridge University Press